Available online at www.sciencedirect.com
SCIENCE DIRECT®
Bioorganic & Medicinal Chemistry Letters 15 (2005) 3778–3781
Bioorganic & Medicinal Chemistry Letters

Discovery and in vitro evaluation of potent kinase inhibitors: Pyrido[1′,2′:1,5]pyrazolo[3,4-*d*]pyrimidines

Michael J. Alberti, Elizabeth P. Auten, Karen E. Lackey, Octerloney B. McDonald, Edgar R. Wood, Frank Preugschat, Geoffrey J. Cutler, Laurie Kane-Carson, Wei Liu and David K. Jung*

GlaxoSmithKline, 5 Moore Drive, Research Triangle Park, NC 27709, USA

Received 28 March 2005; revised 12 May 2005; accepted 16 May 2005
Available online 29 June 2005

Abstract—The discovery, synthesis, potential binding mode, and in vitro kinase profile of several pyrido[1′,2′:1,5]pyrazolo[3,4-*d*]-pyrimidines as potent kinase inhibitors are discussed.

Protein kinases catalyze the phosphorylation of tyrosine and serine/threonine residues in various proteins involved in the regulation of all functions.[1] Protein kinases can be broadly classified as receptor (e.g., EGFr, c-erbB2, PDGFr, and VEGFR2) or non-receptor (e.g., c-src, b-raf, and ZAP70) kinases. Inappropriate or uncontrolled activation of many of these kinases, by over-expression, constitutive activation, or mutation, has been shown to result in uncontrolled cell growth.[2] Drug discovery efforts have targeted this aberrant kinase activity in cancer, asthma, psoriasis, and inflammation, to name a few.[3]

Recent advances in the identification of erbB family kinase inhibitors have created hope for the modulation of uncontrolled cell growth in cancer therapy for solid tumors.[4] For example, the compounds shown in Figure 1, Iressa™ and GW572016, continue to show promising results in clinical trials on cancer patients.[5] Gleevec™'s activity in bcl-abl or c-kit-mediated malignancies is well-documented and CEP1347 looks promising for Parkinson's disease.[6,7] Despite these tremendous results in the development of signaling inhibitors, there remains a gap in the understanding of the selectivity and required inhibition profile of kinase inhibitors to achieve efficacy without introducing toxicity.[8]

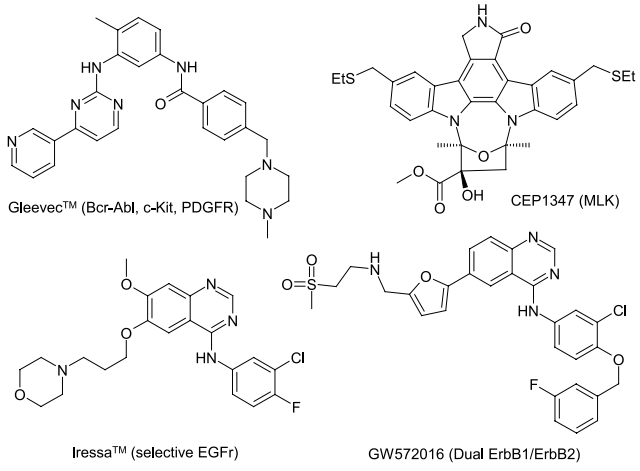

Figure 1. Successful examples of kinase inhibitors that have progressed to clinical trials and patient care.

Herein, we report the generation of a novel scaffold where the substitution pattern targets different regions of the ATP-binding site of the protein kinase domain to create differentially selective molecules. Based on literature reports, linearly fused tricyclic core systems have been used as scaffolds for kinase inhibitors.[9] Our goal was to develop a novel tricyclic core ring system that could be decorated with a variety of diverse substituents to examine their structure–activity relationship (SAR) against a panel of kinase inhibition assays. Herein, we report the results of the utility of this approach to generate useful, selective tool compounds.

Keyword: Kinase inhibitor; VEGFR; GSK; Erb; EGFR.
* Corresponding author. Tel.: +1 919 483 8391; fax: +1 919 483 6053; e-mail: david.k.jung@gsk.com

0960-894X/$ - see front matter © 2005 Elsevier Ltd. All rights reserved.
doi:10.1016/j.bmcl.2005.05.100

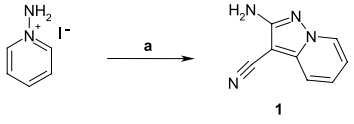

Scheme 1. Synthesis of key intermediate 2-amino-3-cyano-pyrazolo[1,5-*a*]pyridine **1**. Reagents: (a) malononitrile, ethanol, potassium carbonate (25%).

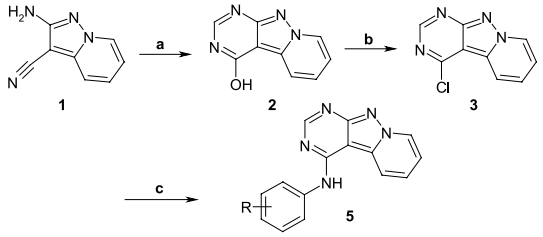

Scheme 2. Synthesis of *N*-phenylpyrido[1′,2′:1,5]pyrazolo[3,4-*d*]pyrimidin-4-amine derivatives **5a**–**d**. Reagents and conditions: (a) formic acid, cat. sulfuric acid, 90 °C; (b) $POCl_3$ (61%, two steps); (c) anilines, *i*-PrOH, reflux.

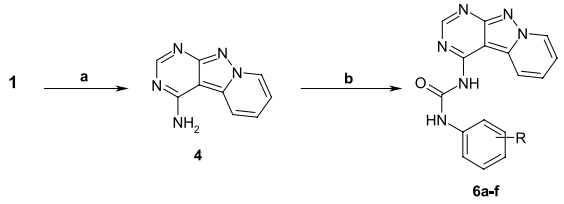

Scheme 3. Synthesis of *N*-phenyl-*N*′-pyrido[1′,2′:1:5]pyrazolo[3,4-*d*]pyrimidin-4-yl-urea derivatives **6a**–**f**. Reagents and conditions: (a) formamide, MW 240 °C (79%); (b) isocyanates, MeCN, 25 °C, 16 h.

The syntheses of two novel classes of kinase inhibitors, *N*-phenyl-pyrido[1′,2′:1,5]pyrazolo[3,4-*d*]-pyrimidin-amine and *N*-phenyl-*N*′-pyrido[1′,2′:1,5]pyrazolo [3,4-*d*]-pyrimidin-4-yl-urea derivatives, are shown in Schemes 1–3.

The key aminonitrile intermediate **1** was synthesized by combining the commercially available *N*-aminopyridinium iodide and malononitrile in ethanol. Heating this mixture with microwave irradiation in the presence of 2 equiv of potassium carbonate generates the desired product. This intermediate has been used to prepare two classes of kinase inhibitors. Preparation of those derivatives with aniline substituents at the 4-position is shown in Scheme 2, and a synthetic approach used to prepare inhibitors with urea substitution at the 4-position is shown in Scheme 3.

The synthesis of anilino-substituted analogs was started by heating the aminonitrile **1** with formic acid in the presence of catalytic sulfuric acid (Scheme 2). The resulting pyrimidinone derivative **2** was converted to the corresponding chloroimidate **3** with phosphorous oxychloride. The final displacement of the chloride with an appropriate aniline was accomplished by heating in isopropyl alcohol to give the desired *N*-phenylpyrido[1′,2′:1,5]pyrazolo[3,4-*d*]pyrimidin-4-amine compounds (**5a**–**d**).

Scheme 3 depicts the sequence of reactions used to prepare urea-substituted derivatives **6a**–**f**. Subjecting the aminonitrile intermediate **1** to microwave irradiation in the presence of formamide results in the formation of tricyclic amine **4**. Stirring this product overnight with an isocyanate in acetonitrile gave the desired *N*-phenyl-*N*′-pyrido[1′,2′:1,5]-pyrazolo[3,4-*d*]pyrimidin-4-yl-urea compounds. The synthetic sequences shown above are amenable to the production of large number of compounds by scaling up key intermediates **3** and **4**, and adding the final diversity in a parallel array format.[10,11]

Compounds **4**, **5a**–**d**, and **6a**–**f** are representative examples of derivatives that can be synthesized by the methods described above. The compounds were evaluated in a panel of kinase enzyme assays and the data for erbB2, EGFR, GSK3, and VEGFR2 are summarized in Tables 1 and 2. The free amino-substituted derivative **4** showed no activity against EGFR, erbB2, GSK3, or VEGFR. However, replacement of the amino substituent with aniline derivatives resulted in potent inhibitors of erbB2 and/or EGFR, with selectivity over GSK3 and VEGFR. The SAR that confers potency and selectivity to the quinazoline series for the erbB family. TK inhibition was evaluated in *N*-phenylpyrido[1′,2′:1,5]pyrazolo[3,4-*d*]pyrimidin-4-amines.[12] For example, **5a** has a 'small' anilino group, and like Iressa™, is selective for EGFR

Table 1. *N*-Phenylpyrido[1′,2′:1,5]pyrazolo[3,4-*d*]pyrimidin-4-amines

Compound	Structure	ErbB2[14]	EGFR[14]
4	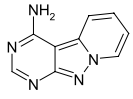	>10	>10
5a	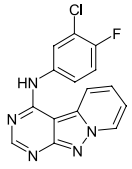	>10	0.200
5b	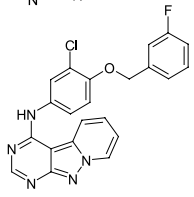	0.063	0.032
5c	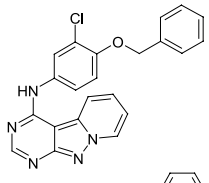	0.200	0.050
5d	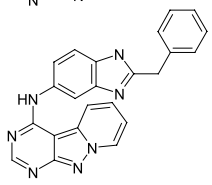	1.58	5.01

Kinase enzyme inhibition expressed as IC_{50} values in micromolar.[14] The IC_{50} values are >10 μM for GSK3 and VEGFR2 for compounds **4** and **5a**–**d**.

Table 2. *N*-Pyrido[1′,2′:1,5]pyrazolo[3,4-*d*]pyrimidin-4-yl-ureas

Compound	Structure	GSK3[15]	VEGFR[16]
6a	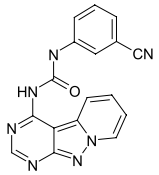	0.126	0.200
6b	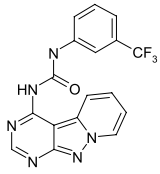	0.158	0.251
6c	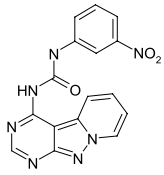	0.316	>10
6d	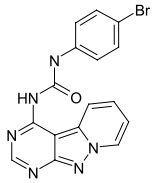	1.00	3.98
6e	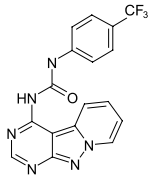	1.58	3.98
6f	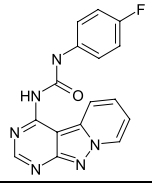	>10	0.631

Kinase enzyme inhibition expressed as IC_{50} values in micromolar.[15,16] The IC_{50} values are >10 μM for ErbB2 and EGFR for compounds **6a**–**f**.

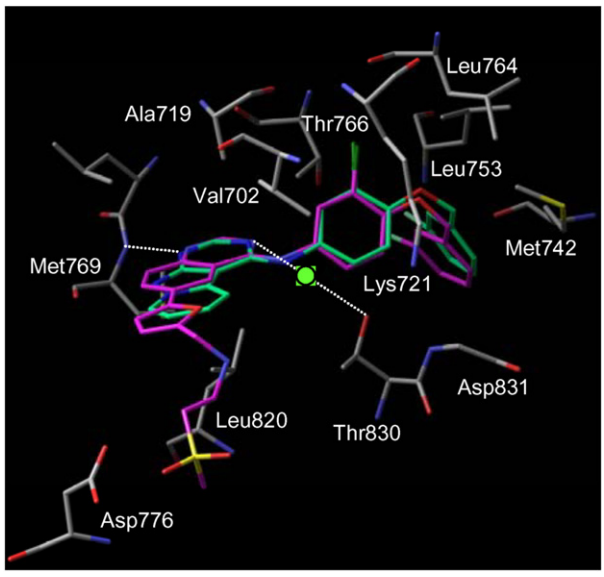

Figure 2. Docking model of **5b** (green), compared with a cocrystal of GW572016 (purple) in EGFR.[8] Hydrogen bonds are indicated by dashed lines.

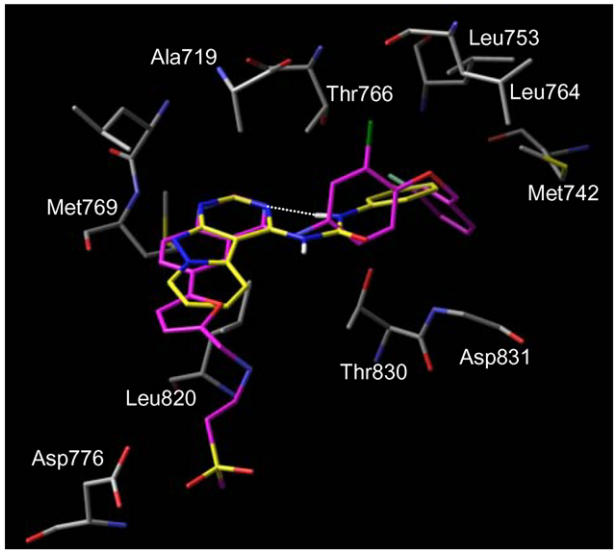

Figure 3. Docking model of **6a** (yellow), compared with a cocrystal of GW572016 (purple) in EGFR.[8] Hydrogen bonds are indicated by dashed lines.

over erbB2. While a larger aniline substituent in **5b**, like GW572016, is a potent dual EGFR/erbB kinase inhibitor (Fig. 2). The potency of this dual inhibition is dependent on substitution on the aniline moiety, and a drop in potency was observed with **5c** and **d**.

To confirm our belief that the novel tricyclic ring system was able to bind in the ATP-binding site of EGFR so that it possessed similar SAR to the quinazolines, we modeled several viable binding modes. The best model is shown in Figure 2 where **5b** is compared with a cocrystal structure of GW572016[8]. The aniline portion of the compounds is overlaid in an identical fashion in the back-pocket region, allowing the N-1 to interact with the hinge region. The tricyclic core then extends down the center of the binding site, which suggests that there is space for 6- and 7-position substitutions for increased interactions.

When the aniline substituent of a pyrido[1′,2′:1,5]pyrazolo[3,4-*d*]-pyrimidine scaffold is changed to an aryl urea, no activity against erbB2 or EGFR is observed. This lack of erbB2/EGFR inhibition from the urea derivatives may be attributed to the fact that a threonine residue exists in the ATP-binding pocket of EGFR and erbB2. This threonine (Thr830) forms a water-mediated hydrogen bond from the quinazoline N-3 nitrogen of GW572016 to the threonine hydroxyl (see Fig. 2). This same interaction could exist with the aniline-substituted pyrido[1′,2′:1,5]pyrazolo[3,4-*d*]pyrimidines.

However, interaction with the urea-substituted derivatives is disrupted by the existence of an intramolecular hydrogen bond between the urea nitrogen and the corresponding nitrogen of the tricyclic core (see Fig. 3).[13] This intramolecular hydrogen bond not only disrupts the interactions with the threonine of EGFR/erbB2, but also slightly changes the relative orientation of the aryl substituents of the aniline and urea derivatives when superimposed on each other.

Although the urea-substituted pyrido[1′,2′:1,5]pyrazolo[3,4-*d*]pyrimidines do not show inhibition of EGFR/erbB2, they do begin to show moderate inhibition against GSK3 and/or VEGFR2 (see Table 2). The range of potencies within the urea-substituted series provides SAR which suggests that this template could be used to develop GSK3 selective compounds (e.g., **6c**) or VEGFR2 selective compounds (e.g., **6f**).

The facile synthesis and kinase inhibition data for the pyrido[1′,2′:1,5]pyrazolo[3,4-*d*]-pyrimidine derivatives demonstrate the potential of this scaffold to generate diverse kinase inhibition profiles. The most obvious trend observed is that the anilino-substituted derivatives demonstrated inhibition of the erbB family, but not GSK3 or VEGFR2, while the reverse trend is observed for the urea-substituted derivatives.

References and notes

1. Jordan, J. D.; Landau, E. M.; Iyengar, R. *Cell* **2000**, *103*, 193.
2. Blume-Jensen, P.; Hunter, T. *Nature* **2001**, *411*, 355.
3. Cohen, P. *Nat. Rev. Drug Disc.* **2002**, *1*, 309.
4. Gschwind, A.; Fischer, O. M.; Ullrich, A. *Nat. Rev. Cancer* **2004**, *4*, 361.
5. Tiseo, M.; Liprevite, M.; Ardizzoni, A. *Curr. Med. Chem.: Anti-Cancer Agents* **2004**, *4*, 139.
6. Giles, F. J.; Kantarjian, H.; Cortes, J. *Expert Rev. Anticancer Ther.* **2004**, *4*, 271.
7. Saporito, M. S.; Hudkins, R. L.; Maroney, A. C. *Prog. Med. Chem.* **2002**, *40*, 23.
8. Wood, E. R.; Truesdale, A. T.; McDonald, O. B.; Yuan, D.; Hassell, A.; Ellis, B.; Pennisi, C.; Horne, E.; Lackey, K.; Alligood, K. J.; Rusnak, D. W.; Gilmer, T. M.; Shewchuk, L. *Cancer Res.* **2004**, *64*, 6652.
9. Showalter, H. D. H.; Bridges, A. J.; Zhou, H.; Sercel, A. D.; McMichael, A.; Fry, D. W. *J. Med. Chem.* **1999**, *42*, 5464.
10. Baindur, N.; Chadha, N.; Player, M. *J. Comb. Chem.* **2003**, *5*, 653.
11. Graveleau, N.; Masquelin, T. *Synthesis* **2003**, *11*, 1739.
12. Cockerill, S. G.; Lackey, K. E. *Curr. Top. Med. Chem.* **2002**, *2*, 1001.
13. Cherry, M.; Williams, D. H. *Curr. Med. Chem.* **2004**, *11*, 663.
14. Compounds were tested for EGFR or ErbB-2 protein tyrosine kinase inhibitory activity in substrate phosphorylation assays using enzymes purified from a baculovirus expression system. Reagent production and assay methodology were conducted essentially as described (Brignola, P. S. et al. *J. Biol. Chem.* **2002**, *277*, 1576). The method measures the ability of the isolated enzyme to catalyze the transfer of the γ-phosphate from ATP onto tyrosine residues in a biotinylated synthetic peptide (biotin-Ahx-RAHEEIYHFFFAKKK-amide). Reactions were performed in 96- or 384-well polystyrene plates in a final volume of 20 or 45 μl. Reaction mixtures contained 50 mM MOPS (pH 7.5), 2 mM $MnCl_2$, 10 μM ATP, 0.125 μCi [γ-^{33}P]ATP per reaction, 2 μM peptide substrate, and 1 mM dithiothreitol. Reactions were initiated by adding 1 pmol (20 nM) per reaction of the indicated enzyme. The reaction was allowed to proceed for 15 min, terminated, and quantified using a scintillation proximity assay procedure as described (McDonald, O. B., Antonsson, B., Arkinstal, S., Marshall, C. J., and Wood, E. R. *Anal. Biochem.* **1999**, *268*, 318).
15. The catalytic domain of vascular endothelial growth factor receptor 2 (VEGFR2) was expressed and purified using methods similar to those described for ErbB-2 and EGFR. Kinase assays were performed as described above with the following modifications: VEGFR2 assays contained 10 nM enzyme, 100 mM HEPES, pH 7.5, 0.1 mg/ml bovine serum albumin, 0.1 mM dithiothreitol, 360 nM peptide A, 75 μM ATP, and 5 mM $MgCl_2$. The reaction was allowed to proceed for 40 min. Product was detected using a homogeneous time-resolved fluorescence procedure (Park, Y.-W., Cummings, R. T., Wu, L., Zheng, S., Cameron, P. M., Woods, A., Zaller, D. M., Marcy, A. I., and Hermes, J. D. *Anal. Biochem.* **1999**, *269*, 94). Briefly, the reactions were quenched by adding 100 μl of 100 mM HEPES, pH 7.5, 100 mM EDTA, 45 nM streptavidin-linked allophycocyanin (Molecular Probes, Eugene, OR), and 3 nM europium-conjugated anti-phosphotyrosine antibody (Wallac, Turku, Finland). The product was detected using a Victor plate reader (Wallac, Turku, Finland) with a time delay at 665 nm.
16. Human GSK3b was expressed in *Escherichia coli* with a 6-His tag at the N-terminus. The protein was purified using metal-chelate affinity chromatography. The incorporation of radioactive phosphate into a biotinylated synthetic peptide, Biotin-Ahx-AAAKRREILSRRP-S(PO3)YR-amide, was detected using a scintillation proximity assay (SPA) method as described above. Assay conditions were as follows: 100 mM HEPES, pH 7.2, 10 mM $MgCl_2$, 0.3 mg/mL heparin sulfate, 0.1 mg/mL BSA , 1 mM DTT , 2.5 μM ATP, 0.6 uCi/rxn ^{33}P labeled ATP, and 1.2 μg/mL GSK-3b protein. The plates are incubated at room temperature for 19 min prior to the addition of SPA stop solution.